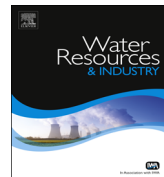Contents lists available at ScienceDirect

Water Resources and Industry

journal homepage: www.elsevier.com/locate/wri

Adsorption studies of arsenic(III) removal from water by zirconium polyacrylamide hybrid material (ZrPACM-43)

CrossMark

Sandip Mandal, Manoj Kumar Sahu, Raj Kishore Patel*

Department of Chemistry, National Institute of Technology, Rourkela, Odisha, 769008, India

ARTICLE INFO

ABSTRACT

A novel hybrid material zirconium polyacrylamide (ZrPACM-43) was synthesized by mixing aqueous solution of zirconium oxychloride and mixture of acrylamide following an environmental friendly sol–gel method. The material was characterized by FTIR, XRD, TGA-DTA, and SEM-EDS. The extent of arsenic removal capacity was tested by the material by varying the solution parameters like adsorbent dose, adsorbate concentration, pH of the solution, contact time and temperature. The maximum removal efficiency of arsenic(III) was 98.22% under optimum conditions with adsorption equilibrium time of 120 min. The adsorption process followed second order kinetics and adsorption data were best fitted to linearly transformed Freundlich isotherm with correlation coefficient of $R^2 > 0.999$. Adsorption capacity (q_o) calculated from Langmuir isotherm was found to be 41.48 mg g^{-1}. The thermodynamic parameter ΔH indicates an endothermic adsorption process. The regeneration study shows that the material is regenerated by 1 M alkali solution.

© 2013 The Authors. Published by Elsevier B.V.

1. Introduction

The use of heavy metals and their compounds has increased the comfort of human being in great way. They are used in different processes [1]. The excessive use of heavy metals and metalloids causes to increase

---

* Corresponding author. Tel.: +91 0661 246 2652, +91 9437245438, +91 9778212090; fax: +91 661 246 2651.
  E-mail addresses: sandipmandal9@gmail.com (S. Mandal), rkpatel@nitrkl.ac.in, rkpatelnitr@gmail.com (R.K. Patel).

their concentration in aquatic systems. Arsenic is a metalloid, a known poison element, and exists as oxide or anion and known to be 20th most abundant element in the earth [1]. The presence of arsenic in water is due to natural weathering process, geochemical reactions, biological activity, combustion of fossil fuels, volcanic eruptions, gold mining, leaching of man-made arsenic compounds, smelting of metals ores, desiccants, wood preservatives, agricultural pesticides and many other anthropogenic activities [1–3]. Arsenic generally occurs as arsenic(V) and (III), depending on pH and redox conditions [1,4,5]. Arsenic(III) is more toxic than arsenic(V), because arsenic(III) binds to single but with higher affinity to vicinal sulfhydryl groups that reacts with a variety of proteins and inhibits their activity [6]. Arsenic(III) is more stable than As (V) because of electronic configuration. Long term ingestion of arsenic contaminated drinking water causes skin lungs and kidney cancer, gastrointestinal disease, bone marrow disorder, cardiovascular diseases and other diseases [7]. Due to extreme toxicity of arsenic in drinking water, World Health Organization (WHO, Geneva, Switzerland), Environmental Protection Agency (US-EPA, United States) [8,9] and Central Pollution Control Board (CPCB, India) [10,11] has set 0.01 mg L^{-1} and 0.05 mg L^{-1} as maximum permissible limit of arsenic in drinking water. Many conventional processes for treatment of arsenic like adsorption [12,13], coagulation [12], co-precipitation [14], ion-exchange [15–18] and oxidation-reduction process have been reported. Among all the process, the adsorption is one of the promising methods [12]. The aim of this work is to synthesize environment friendly hybrid material in lab scale and to study in detail for removal efficiency of arsenic(III) from water by using the material. The main objectives are: (a) synthesis and characterization of the hybrid material zirconium polyacrylamide, (b) to determine the kinetic parameter of arsenic(III) adsorption, and (c) to study the effect of temperature, pH, time, initial concentration and coexisting ions on the arsenic(III) adsorption. The present material which is synthesized in lab scale and subsequently utilized for removal of arsenic(III) from water is not reported anywhere in the literature. This is a novel environment friendly hybrid material which can be utilized in small scale to large scale water treatment for arsenic removal.

2. Materials and methods

2.1. Reagents and chemicals

All chemicals were used of analytical range (AR grade), which are obtained from E. Merck (Merck, India), Sigma-Aldrich (Sigma-Aldrich, United States), and Loba Chemie (Loba Chemie, India). Zirconium oxy chloride (purity ≥ 99.0%), ammonium persulfate (purity = 98%), bis-acrylamide (purity = 97%), hydroxy-methyl aminomethane (TRIS, purity ≥ 99.8%), tetramethyl ethylenediamine (TEMED, purity ≥ 99.5%), and arsenious oxide (purity ≥ 99.9%), were used without further purification for the synthesis and experiments, borosil glassware was used to conduct all the experiments. All solutions are prepared in distilled water. 1 L stock solution of arsenic(III) was prepared by dissolving 1.320 g arsenic trioxide (As_2O_3) in water containing 4 g sodium hydroxide (NaOH) and diluted to 1 L; 1.00 ml = 1.00 mg arsenic(III), standard arsenic(III) solution were prepared for analysis by serial dilution of stock solution on daily basis.

2.2. Synthesis of zirconium polyacrylamide

Zirconium polyacrylamide was synthesized in the laboratory by the sol–gel method with water as a solvent by the following procedure. 52.8 ml of distilled water with 20 ml of 30% acrylamide mixture (acrylamide + bis-acrylamide) was taken, in a 250 ml round bottom flask, 15 ml of 1.5 M TRIS was added to maintain the pH 8.8 and 10 ml of 10% of zirconium oxychloride was added to the above solution with constant stirring. To this mixture, 1 ml of 10% ammonium persulphate and 0.2 ml of TEMED as a catalyst and reaction initiator was added drop wise sequentially with vigorous stirring to make a net volume of 100 ml. A white colored gel was formed, which was allowed for ageing at room temperature for 12 h. Then it was filtered and washed several times with distilled water to remove excess reagent. The material is dried at 50 °C for 2 h in a hot air oven till it forms white granules. Finally the materials were kept in an air tight bottles until used. A series of same material was prepared by varying the precursor's molar concentration and the best material having the lowest

Table 1
Different composition of the hybrid material ZrPACM, surface area and particle size studies.

Material composition	Molar ratio	Particle size (nm)	Surface area (m²/g)
ZrPACM-78	1:1	78.33	178.71
ZrPACM-82	1:3	82.64	158.13
ZrPACM-43	2:1	43.67	341
ZrPACM-66	2:3	66.27	194.02
ZrPACM-62	3:1	62.78	223
ZrPACM-53	3:3	53.20	278.33

particle size is obtained when the molar ratio is 2:1 (acrylamide mixture:ZrOCl$_2$) and represented as ZrPACM-43, which was taken for further optimization and removal studies (Table 1).

2.3. Characterization

The zirconium polyacrylamide was characterized by using various analytical instruments. Surface morphology of the material was examined using SEM (JEOL, JSM 6390LV, Japan) coupled with EDX (JEOL, JSM-6480LV) technique at an accelerating voltage of 20 kV. The surface charge density (σ) of sorbent was determined by a potentiometric titration method. The following equation was used to determine the surface charge density:

$$\sigma_o = ((C_A - C_B + [OH^-] - [H^+])F)/m \tag{1}$$

where C_A and C_B were the molar concentrations of acid and base needed to reach a point on the titration curve, [H$^+$] and [OH$^-$] were the concentrations of H$^+$ and OH$^-$, F was the Faraday constant (96,490 C mol^{-1}), m (g) was the mass of the sorbent. Surface area and pore volume were measured using a BET (Quantachrome Autosorb I, Boynton Beach, Florida) in N$_2$ atmosphere by adsorption and desorption technique. X-ray diffraction (XRD) data were obtained by a diffractometer by using PHILLIPS X'PERT X-ray diffractometer model PW 1830 (Almelo, Netherlands) with CuK radiation (35 kV and 30 mA) at a scan rate of 3°/min and was analyzed using standard software provided with the instrument. FTIR spectrometer spectrum RX I (Perkin-Elmer corporation, USA) are used to know various functional group of the adsorbent. FTIR were recorded at in 400–4000 cm^{-1} with a resolution of 4 cm^{-1} and 64 scans. Particle size was analyzed by Malvern Nano ZS 90 (Malvern, UK). The thermogravimetric analysis was carried out with a DTG-60 (DTG-60, Shimadzu corporation, Japan) in nitrogen atmosphere under a flow of 30 ml min^{-1} and heating rate of 10 °C min^{-1} varying the temperature from 25 °C to 800 °C. The total arsenic concentration was determined by using hydride generation technique and flame photometer technique of AAS (Elico SL 176, India) using hollow cathode lamp (HCL) at wavelength range of 193.7–197.2 nm at slit width of 2.5 nm with EHT of 700 V and maximum current of 7.0 mA.

2.4. Adsorption Experiments

The extent of arsenic(III) removal was studied using batch mode of experiment which was carried out by mixing adsorbent with fixed volume of arsenic(III) solution in 250 ml stopper glass bottle. Stoppers were used to avoid change in concentration due to evaporation. The mixture was agitated at 400 r min^{-1} in a mechanical shaker (Remi Equipments, Mumbai, India) placed in an incubator, until equilibrium was attained. After a predetermined contact time, the aqueous samples in each bottle were decanted and centrifuged at 4500 r min^{-1} for 5 min and filtered through Whatman-42 filter paper (pore size: 2.5 μm) and the arsenic concentration in the filtrate was measured using an atomic adsorption spectrophotometer (AAS). The experiments were conducted at variable dose (0.1–1.5 g/100 mL), pH (1–12), contact time (10–140 min), temperature (20–80 °C), and initial concentration (10–270 mg L^{-1}). Where the optimum experimental conditions were ascertained, arsenic uptake by the adsorbing material was calculated using the following equation:

$$Q_e = (C_0 - C_e)V/W \tag{2}$$

where Q_e is equilibrium uptake (mg g^{-1}), V is the volume of solution (L). C_0 (mg L^{-1}) is the initial concentration of arsenic(III), C_e (mg L^{-1}) is the concentration of arsenic(III) at equilibrium time "t" and W is the mass of the adsorbent material (g). In order to know the effect of other competing ions on arsenic(III) adsorption, studies were done by using anions (bicarbonate, carbonate, sulfate and nitrate). Solutions of these anions were prepared from their sodium and potassium salts. The initial concentration of arsenic(III) was fixed at 10 mg L^{-1},while the initial concentration of other anions varied from 10 mg L^{-1}to 270 mg L^{-1}. The best fit models and error analysis of the present studies were done by using Origin pro (version 8, origin lab corporation, USA) and MS-Excel (version 2010, Microsoft, USA) software. The best fit was disused using error bar plot, regression correlation coefficient (R^2), standard deviation (SD) and chi-square analysis (χ^2).

3. Results and discussion

3.1. Characterization

The material is chemically stable as it is not soluble up to 3 M solution of mineral acids (H$_2$SO$_4$, HNO$_3$ and HCl) and alkali (NaOH, NH$_4$OH and KOH). The experiment was conducted in 30 ml of different mineral acids and alkali of different molar concentration for 24 h and supernatant liquid is collected by filtration and analyzed for zirconium. The scanning electron microscopy with corresponding EDS of material with and without arsenic loaded are presented in Fig. 1. The energy dispersive spectrum (EDS) in the Fig. 1 shows the elemental composition of the material. There is a
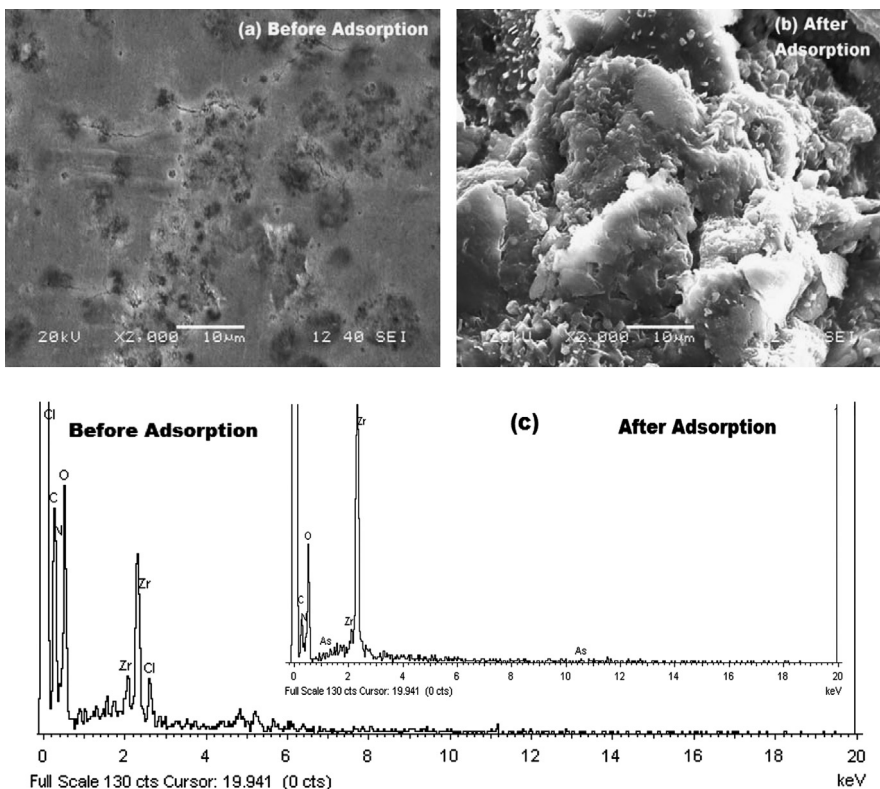

Fig. 1. SEM and EDS of hybrid material ZrPACM-43: (a) before adsorption (b) after adsorption and (c) EDX micrographs of before adsorption and after adsorption.

remarkable change in the morphology and structure of the material when loaded with arsenic. It is clearly observed that crystals are embedded in the surface of the material after loaded with arsenic. The micrograph shows surface heterogeneity resulted from the adsorption of arsenic(III) on the surface. The corresponding EDS spectrum indicates the presence of C, O, Zr and As. BET surface area of the material is found to be 341 $m^2 g^{-1}$. Powdered XRD diffractogram was studied with PCPDFWIN and Philips X'pert high score software to search for the phases of starting materials and adsorbed materials, powdered XRD diffractogram of the material before adsorption and after adsorption is represented in Fig. 2(a) and (b). Few sharp peaks are observed before and after indicating the sample is crystalline in nature. The normal crystallite sizes of material were calculated using the Debye Scherrer equation [19]

$$D_{(011)(220)} = 0.9\lambda/(\beta_{2\theta} \cos \theta_{max})$$ (3)

where D (plane of reflection at before adsorption (0 1 1) and after adsorption (2 2 0)) is the average crystal size in nm, λ is the specific wavelength of X-ray used, θ is the diffraction angle and $\beta_{2\theta}$ is the angular width in radians at intensity equal to half of the maximum peak intensity. The crystallite size was found to be 53.60 nm and 238.00 nm before and after adsorption respectively, exact composition were drawn and compared by ICCD Database 1998 and represented in Fig. 2(a) and (b). The increment in the crystallite size is may be due to increment in space charge polarization and crystal defects after adsorption. FTIR studies were done in order to know the functional groups and structure of the present material. The spectrum of before adsorption and after adsorption is represented in Fig. 3 (a) and (b). The presence of band at 3414.58 cm^{-1} is due to bonded OH groups, which indicates the presence of water of crystallization. The NH_2 stretching is overlapped with the band with a formation of spike; this peak is shifted to 3439.28 cm^{-1} after adsorption may be due to coordination of arsenic (III) with NH groups. The presence of next band at 2882.01 cm^{-1} in material is due to presence of amide group which is shifted to 2994.19 cm^{-1} with slight broadening after adsorption. The peak at 2818.95 cm^{-1} is due to combined stretching of N–H and O–H groups, the peak further shifted after adsorption. The peak at 1612.42 cm^{-1} is due to C=O stretching groups present in the structure, the peak at 1200.00 cm^{-1} in the material is assigned to C–H and C–C stretching, the presence of peak at finger print region 798.06 cm^{-1} and 618.35 cm^{-1} is due to C–N stretching and metal–oxygen bonding which is shifted to 745.88 cm^{-1}, 618.73 cm^{-1} and 521.73 cm^{-1} after adsorption indicates the adsorption of arsenic. The TGA-DTA analysis of the material is presented in Fig. 4. The weight loss occurred in the following three steps: (1) in the temperature range of 30–250 °C (21.37%) is due to loss of physical adsorbed water; (2) 53.74% in the temperature range of 250 °C to 580 °C is attributed mainly to the loss of lattice water and NH_2 groups; and (3) 50.77% at higher temperature (580–700 °C) might be due to structural deformation, the DTA curve supported the above finding.
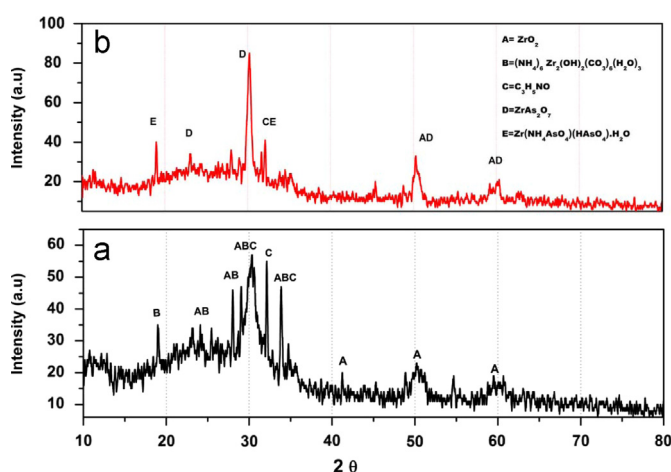

Fig. 2. X-ray diffraction pattern of hybrid material ZrPACM-43: (a) before adsorption and (b) after adsorption of arsenic(III).
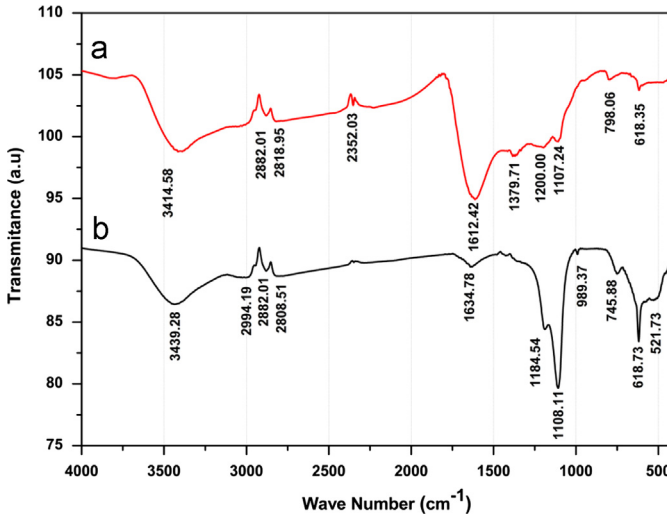
Fig. 3. FTIR spectrum of hybrid material ZrPACM-43: (a) before adsorption and (b) after adsorption of arsenic(III).
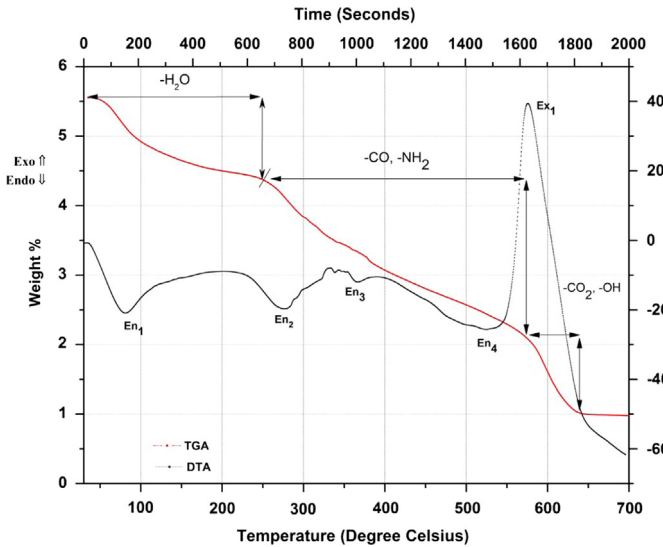

Fig. 4. Thermogravimetric analysis and differential thermal analysis of hybrid material ZrPACM-43.

The fresh adsorbent was analyzed to obtain its elemental composition by CHNS Elementar and EDS. The results indicate the elemental composition as Zr 16.82%, O 28.08%, C 14.80%, H 3.11%, and N 2.88%, and others 34.31%. Based on the above studies of FTIR, TGA-DTA and the elemental analysis, the molecular formula of the adsorbent was deduced by using the Alberti equation [20].

$$18n = X(M + 18_n)/100 \qquad (4)$$

where X is the percent of water content and $(M + 18)$ is the molecular weight of the material. It gives the value of "n" as 2.40, the tentative empirical formula for the material can be suggested as $[(ZrO_2) (C_4H_7NO)] \cdot nH_2O$. The zero point surface charge density of the hybrid material as a function of pH is studied and represented in Fig. 5. The study shows that the surface holds positive charge in lower
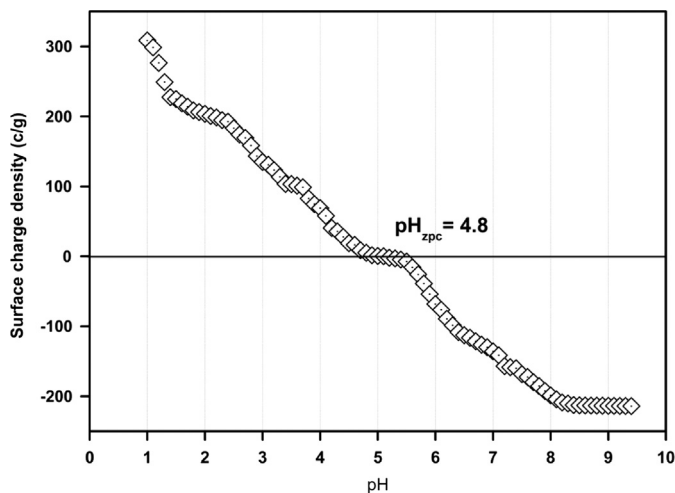
Fig. 5. Surface charge density as a function of pH ($m = 1$ g L^{-1}) for hybrid material ZrPACM-43.

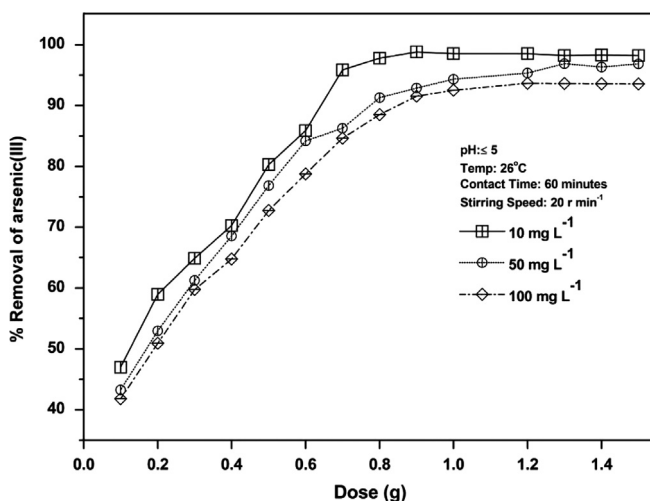**Fig. 6.** Variation of adsorbent dose on the percentage removal of arsenic(III) by the hybrid material. Experimental conditions: pH $\leq$ 5, temperature: 26 °C, contact time: 60 min, and stirring speed: 20 r min^{-1}.

pH value, the surface charge density decreases when the solution pH increases. The pH of zero point surface charge density was recorded around 4.8 (pH$_{zpc}$). The value of pH$_{zpc}$ is positive as solution pH is less than 5, however the surface acquires negative charge as the solution pH is higher than 5.

3.2. Effect of adsorbent dose, pH, and initial arsenic concentration on the removal of arsenic (III)

The effect of adsorbent dose on removal of arsenic(III) was studied at pH $\leq$ 5, stirring speed of 20 r min^{-1} at temperature 26 °C and represented in Fig. 6. As expected the removal of arsenic(III) increases from "47% to 98.22%, 43.25% to 96.87% and 41.79% to 93.56%" with increase in adsorbent dose from 0.1 to 1.5 g/100 ml respectively at a selected contact time of 60 min keeping initial solute concentration at 10 mg L^{-1}, 50 mg L^{-1} and 100 mg L^{-1}. It is found that after dosage of 13 g L^{-1}, there is no significant change in percentage removal of arsenic. The increase in percentage removal could be

attributed to the availability of more number of adsorption sites at the solid phase. Availability of specific surface area and micropore volume plays a vital role for surface adsorption process. However, in present investigation, with further increase in adsorbent dose, the removal extent remains almost constant indicating the saturation of adsorption sites. The saturation of the active sites may also be due to the overlapping of active sites at higher dosage as well as the decrease in the effective surface area resulting in the accumulation of exchanger particles. So, 13 g L^{-1} is considered as the optimum dose and is used for further study.

Percentage removal of arsenic at different pH (1–12) was studied using 13 g L^{-1} of adsorbent dose at room temperature (26 °C), and contact time of 60 min for initial arsenic(III) concentration of 10 mg L^{-1}, 50 mg L^{-1}, and 100 mg L^{-1}. The results are presented in Fig. 7. There is no change in the solution pH after addition of adsorbent and solution remains at pH 7. It is evident from the graph that the highest removal is "97.06% for 10 mg L^{-1}, 94.84% for 50 mg L^{-1} and 87.62% for 100 mg L^{-1} respectively" at pH $\leq$ 5. The removal of arsenic decreases with increase in pH may be due to the followings. (1) When the concentration of H$^+$ ions is more in water solution, then the magnitude of positive charge over amino group is more and (2) competition for active sites by excessive amount of hydroxyl ions present in the water in alkaline pH [21], the above attained pH indicates a good agreement with zero point surface charge (pH$_{zpc}$) study.

3.3. Contact time and adsorption kinetic studies

The effect of contact time on the removal of arsenic(III) was studied in the range of 10 min to 140 min by using 13 g L^{-1} of adsorbent at room temperature (26 °C), at pH $\leq$ 5. From the Fig. 8, it is understood that the effective removal achieved within 120 min, which is "98.67%, 96.32% and 92.67%" for initial concentration of 10 mg L^{-1}, 50 mg L^{-1} and 100 mg L^{-1} respectively. After 120 min there is no change in removal percentage, so 120 min was considered as the effective equilibrium time for adsorption. Initially the rate of removal is higher, which may be due to more vacant sites for adsorption in the adsorbent and having high solute concentration gradient.

In order to examine the controlling mechanisms of adsorption process such as mass transfer and chemical reaction, several kinetic models like Lagergren first order rate equation and second order rate equation are used to test the experimental data using initial concentration of 10 mg L^{-1}, 50 mg L^{-1} and 100 mg L^{-1}. The integrated linear pseudo-first order rate equation and second order
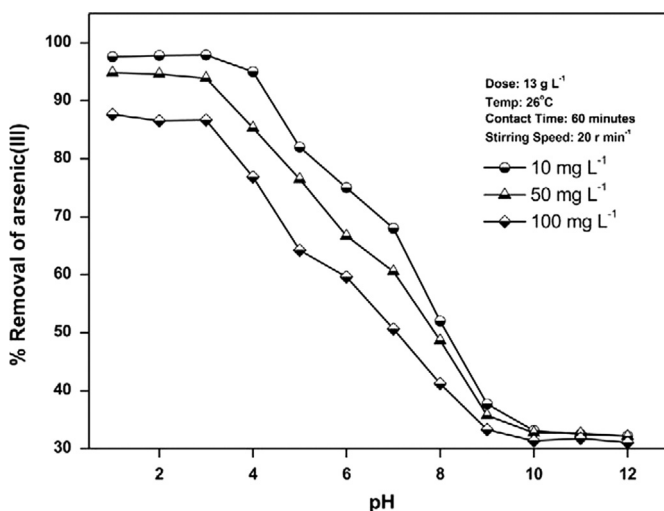

Fig. 7. Effect of pH on the removal of arsenic(III) by hybrid material ZrPACM-43. Experimental conditions: dose: 13 g L^{-1}, temperature: 26 °C, contact time: 60 min, and stirring speed: 20 r min^{-1}.
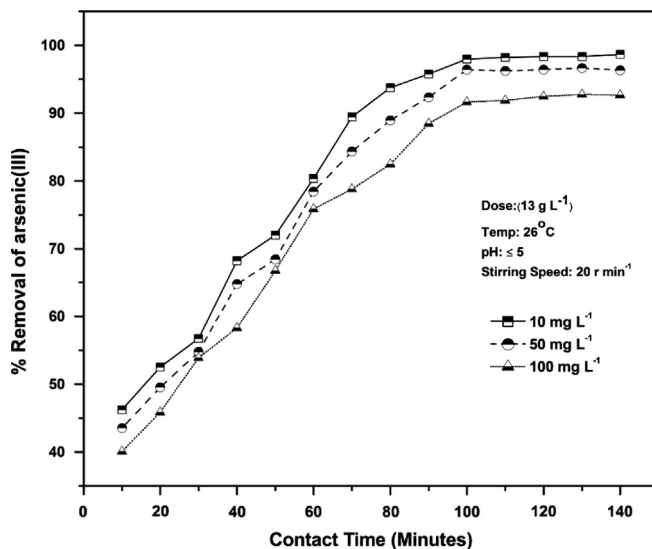
Fig. 8. Effect of contact time on the removal of arsenic(III) by hybrid material ZrPACM-43. Experimental conditions: dose: 13 g L^{-1}, temperature: 26 °C, pH ≤ 5, and stirring speed: 20 r min^{-1}.

Table 2
Rate constants (K_1), and (K_2), were obtained from the graph for removal of arsenic(III) by hybrid material at different initial concentrations.

		Pseudo first order			Second order			
		K_1	R^2	SD	K_2	q_c	R^2	SD
ZrPACM-43	10 mg L^{-1}	0.04	0.99	0.03	1.57	1.57	1.00	0.01
hybrid material	50 mg L^{-1}	0.04	0.92	0.08	0.12	7.79	1.00	0.03
	100 mg L^{-1}	0.05	0.92	0.11	0.07	15.37	1.00	0.15

rate equation are represented as [22,23]

$$\text{Log}(q_e - q_t) = \text{Log } q_e - K_1\{t/2.303\} \tag{5}$$

$$t/qt = [1/(K_2 q_c^2) + 1/q_c]t \tag{6}$$

where q_e and q_t (both in mg g^{-1}) are the amount of arsenic(III) adsorbed at equilibrium and at time "t" respectively, K_1 is adsorption rate constant of pseudo-first order adsorption, K_2 is the rate constant of second order rate equation (g mg^{-1} min^{-1}), and q_c is the maximum adsorption capacity (mg g^{-1}) for the second order adsorption. The values obtained from the plots were represented in Table 2.

3.3.1. The best fit model

The evaluation of the best active kinetic models for fitting the adsorption data was made by standard deviation (SD) and correlation coefficient (R). The SD values and correlation coefficient of material for all kinetic models are shown in Table 2. Lower SD values and good correlation coefficient were observed for second order kinetic model, which indicates the best fit model and significant in describing the arsenic(III) adsorption process.

3.4. Effect of temperature

The effect of temperature upon adsorption process was studied with variation of temperature from 20 °C to 80 °C. Various thermodynamic parameters such as ΔG^T, ΔS^T and ΔH^T were also calculated. The experimental observation indicated that within the range of study, the percentage of uptake of arsenic (III) by the adsorbent material increases from "67.28% to 97.33%, 60.02% to 94.87% and 55.40% to 90.57%" for initial concentration of 10 mg L^{-1}, 50 mg L^{-1} and 100 mg L^{-1} respectively. The highest removal efficiency was at 50 °C for all the initial concentration, which is considered as optimum temperature. The thermodynamic feasibility of adsorbent–arsenic interaction process can be represented as [24,25]

$$\Delta G^0 = -RT \ln K_c \tag{7}$$

$$K_c = C_a/C_i \tag{8}$$

$$\text{Log } K_c = [(\Delta S^T)/R - (\Delta H^T)/RT] \tag{9}$$

$$\Delta G^T = \Delta H^T - T\Delta S^T \tag{10}$$

where C_a and C_i are the amount of arsenic(III) ion adsorbed per unit mass of adsorbent and concentration of arsenic(III) ion in aqueous phase, K_c is the equilibrium constant, R is the universal gas constant (8.314 J mol K^{-1}), T is the temperature (K), ΔG^T, ΔS^T and ΔH^T are the changes in Gibb's free energy, entropy and enthalpy of adsorption respectively. The value of ΔH^T and ΔS^T were evaluated from the slope and intercept of the plot log K_c versus $1/T$. The results of analysis are represented in Table 3. The negative values of ΔG^T at all temperature confirm the spontaneous nature of adsorption. The positive values of ΔH^T confirm the feasibility of the reaction and indicate the endothermic nature of adsorption. The decreasing value of ΔG^T with temperature shows the reaction is more feasible at higher temperature.

3.5. Adsorption isotherm

The relationship between the equilibrium of arsenic(III) adsorbed and the solute concentration was verified using various isotherms. In the present work three isotherm models i.e. Langmuir, Freundlich, and Dubinin–Radushkevic (D–R) were used to find the best fitted model. The studies were done at dose of 13 g L^{-1}, temperature of 50 °C, time of 120 min and at pH $\leq$ 5. The linearized form of the Langmuir, Freundlich and D–R is given below [26–28].

Langmuir model (linear)

$$1/q_e = 1/(q_0 b C_e) + 1/q_0 \tag{11}$$

where, q_e is the amount of arsenic(III) adsorbed at equilibrium (mg g^{-1}), C_e is the equilibrium adsorbate concentration (mg L^{-1}), the values of Langmuir constants b (binding energy constant) and q_o (mono layer adsorption capacity in mg g^{-1}) relates to the energy and capacity of adsorption process. The isotherm criterion can be described by another dimensionless constant, which is otherwise known

Table 3
Thermodynamic parameters for arsenic(III) removal by hybrid material.

		ΔH^T (kJ mol^{-1})	ΔS^T (kJ K^{-1} mol^{-1})	ΔG^T						
				10 °C	15 °C	20 °C	25 °C	30 °C	35 °C	40 °C
ZrPACM-43	10 mg L^{-1}	140	0.383	−136.2	−134.3	−132.3	−130.4	−128.5	−126.6	−124.7
hybrid	50 mg L^{-1}	144	0.257	−141.7	−140.4	−139.1	−137.8	−136.5	−135.2	−133.9
material	100 mg L^{-1}	149	0.364	−145.4	−143.5	−141.7	−139.9	−138.1	−136.2	−134.4

as separation factor or equilibrium parameter r as represented in the following equation:

$$r = 1/(1 + bC_0) \tag{12}$$

where C_0 is the initial concentration of arsenic(III) (mg L^{-1}) and r is the Langmuir isotherm constant. The feasibility of isotherm can be evaluated from the values of r, where $r < 1$ represents favorable adsorption and $r > 1$ represents unfavorable adsorption processes. The calculated value of r for the initial arsenic(III) concentration of 10 mg L^{-1}, 50 mg L^{-1} and 100 mg L^{-1} was found to be 0.07, 0.014 and 0.007 respectively. The adsorption capacity was found to be 41.48 mg g^{-1} obtained from the linear plot of $1/q_e$ versus $1/C_e$.

Freundlich model (linear)

$$\text{Log } q_e = \text{Log } K_f + 1/(n \log C_e) \tag{13}$$

where Freundlich constants K_f and $1/n$ are the adsorption capacity and adsorption intensity respectively represented in Table 4. The values were obtained from the linear plot of $\log q_e$ versus $\log C_e$ and represented in Fig. 9. Higher the value of $1/n$, the higher will be the affinity between the adsorbate–adsorbent and the heterogeneity of the adsorbent sites. In present investigation, the calculated value of $1/n$ was found to be 0.804 indicating that it is valid for the active adsorption sites and contain equal energy for adsorption process as studied by using the D–R model (linear)

$$\ln q_e = \ln q_m - K_\varepsilon^2 \tag{14}$$

$$\varepsilon = RT \ln(1 + 1/C_e) \tag{15}$$

$$E = -(2K)^{(-1/2)} \tag{16}$$

where ε is Polanyi potential, q_m is the hypothetical adsorption capacity, K is the constant related to adsorption energy, R is the universal gas constant (8.314 J mol^{-1} K^{-1}) and T is the temperature in Kelvin, represented in Fig. 10. The value of K and q_m, respectively, is obtained from the slope and intercept of the

Table 4
Various isotherm parameters for removal of arsenic(III) by hybrid material.

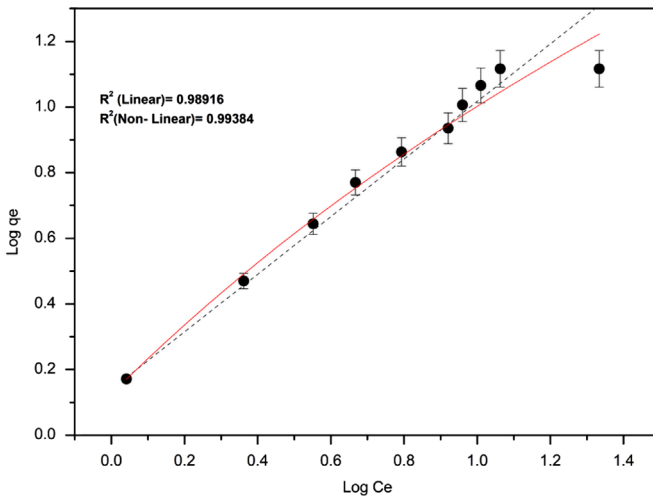| Isotherm models	ZrPACM-43 hybrid material	
	Parameters	Values
Langmuir isotherm constants	q_o (mg g^{-1})	41.49
	b (L mg^{-1})	1.40
	R^2	
		0.951
		0.941
	χ^2	5.28
Langmuir dimensionless equilibrium parameter (r)	10 mg L^{-1}	0.07
	50 mg L^{-1}	0.014
	100 mg L^{-1}	0.007
Freundlich isotherm constants	K_f (mg g^{-1})	0.20
	N	1.24
	R^2	
		0.989
		0.993
	χ^2	1.16
D–R isotherms	K (mol^2 kJ^{-2})	8.07×10^{-7}
	q_m (mg g^{-1})	0.80
	E (kJ mol^{-1})	787.01
	R^2	
		0.903
		0.997
	χ^2	0.42

Fig. 9. Freundlich adsorption isotherm study for the arsenic(III) removal by hybrid material ZrPACM-43. Experimental conditions: dose – 13 g L^{-1}, temperature – 50 °C, contact time – 120 min, stirring speed – 20 r min^{-1}, and pH $\leq$ 5.
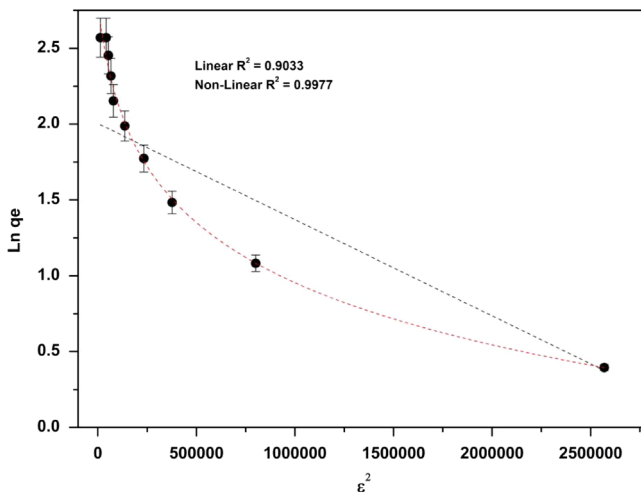

Fig. 10. D–R adsorption isotherm, for arsenic(III) removal by hybrid material ZrPACM-43, Experimental conditions: dose – 13 g L^{-1}, temperature – 50 °C, contact time – 120 min, stirring speed – 20 r min^{-1}, and pH $\leq$ 5.

plot q_e versus ε^2. The value of K was found to be 8.07×10^{-7} mol^2 kJ^{-2} and that of q_m was 0.8026 mg g^{-1}, the mean free energy of adsorption (E) was calculated from the constant K using the relation.

The value of E is very useful in establishing the type of adsorption. The values originate in the present experiment was 787.011 kJ mol^{-1} which is higher than 400 kJ mol^{-1}, and which indicates the present process is chemisorption.

3.5.1. The best fit model

The best fit model for the isotherm studies were calculated by correlation coefficient and Chi-square analysis. However the data are calculated by using the software. The results of correlation coefficient and Chi-square analysis were represented in Table 4. The lower χ^2 and good correlation coefficient values of Freundlich and D–R suggest the applicability of the best fitting model for the adsorption of arsenic on ZrPACM-43 hybrid material, then Langmuir.
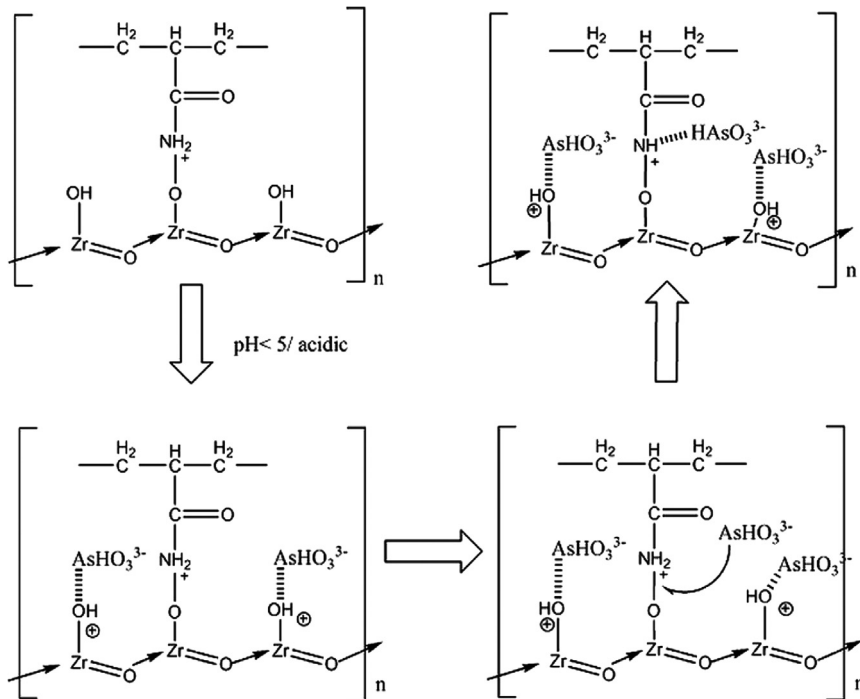
3.6. Mechanism of adsorption of arsenic(III) on ZrPACM-43 hybrid material

A mechanism for the adsorption of arsenic(III) by hybrid material has been proposed by taking the results obtained from the experimental findings and computing the results using mathematical/theoretical models. The mechanism of arsenic removal by the hybrid material was governed by electrostatic adsorption and complexation for which a mechanism is proposed as represented in Fig. 11. At acidic pH, the material gets positively charged due to the protonation of amino groups which remove hydrogen arsenite ion by means of acidic solution which demonstrates a positive redox potential ($+0.6$ V), On the variation of pH, these surface active OH groups may further bind or release H^+ where the surface remains positive due to the following reaction:

$$MOH + H_3O^+ \rightarrow MOH_2 + H_2O \tag{17}$$

The above reaction indicates that the removal efficiency of the material is more at low pH. Thus, when $pH \leq 5.00$, the overall arsenite adsorption mechanism can be represented in two different forms:

(a) Electrostatic interaction between positively charged center (nitrogen) and negatively charged arsenite molecule in solution (Eq. (18)).
(b) Electrostatic attraction and complexation between positively charged surface hydroxyl group and arsenite (Eq. (19)).

$$MNH_2^+ + HAsO_3^{3-} \rightarrow MNH_2^+ - HAsO_3^{3-} \tag{18}$$

$$MOH + H_3O^+ + HAsO_3^{3-} \rightarrow MOH_2^+ - HAsO_3^{3-} + H_2O \tag{19}$$

Proposed Mechanism for Arsenic Adsorption by Hybrid Material

Fig. 11. Proposed mechanism for arsenic(III) removal by hybrid material ZrPACM-43.

This information was supported by the formation of arsenic(III) complexes which is colorless. The presence of arsenic peak in the EDS and XRD spectra of arsenic sorbed hybrid material confirms the occurrence of arsenic sorption onto the hybrid materials.

The modeling of the specific adsorption of arsenic(III) on any material surface depends on a number of external factors such as temperature, pH, initial concentration, as well as the density of surface functional groups available for coordination. In light of the above-mentioned mechanism of adsorption, it may be further noted that the material showed adsorption capacity at a wide acidic pH range, which could be useful for commercial exploitation purpose; a comparative study is represented in Table 5 for removal of arsenic(III) by different hybrid materials and composites reported in the literature.

3.7. Effect of competitive ions and regeneration of adsorbent

The effect of various diverse ions/competing co-ions upon adsorption of arsenic were investigated using chloride, bicarbonate, nitrate, sulfate. The experimental condition for initial arsenic(III) concentration was kept at $10 \, mg \, L^{-1}$ varying the initial concentration of anions from $10 \, mg \, L^{-1}$ to $270 \, mg \, L^{-1}$. It was observed that presence of all these anions reduces the adsorption process. The reduction on adsorption follows the following order by anions sulfate > chloride > carbonate > bicarbonate > nitrate. These ions may be competing for the active sorption sites along with the arsenic during adsorption process which resulted in decrease in adsorption capacity. Apart from this, the effect of these anions towards adsorption may be due to their affinity towards the adsorbent material. Regeneration studies were carried out in order to know the reusability of the hybrid material. The regeneration percentages and reusability of the hybrid material are represented in Fig. 12(a) and (b). Percentage regeneration of the adsorbed arsenic(III) in aqueous solution resulted about 99.78%, 94.51% and 90.12% at pH 10 for initial concentration of $10 \, mg \, L^{-1}$, $50 \, mg \, L^{-1}$ and $100 \, mg \, L^{-1}$ respectively, which indicate that the material can be easily regenerated by alkali and used for several cycles. The reusability studies of the material were done and it was found that the material can be reused up to eight cycles (60% removal).

4. Conclusion

In this study a new zirconium polyacrylamide a novel hybrid material is used for the removal of arsenic(III) from synthetic water. The SEM, EDS, XRD and FTIR analysis confirms the arsenic adsorption; the TGA-DTA reveals that the material is stable up to 680 °C. The lowest particle size

Table 5
Various hybrid materials/composites and there arsenic removal capacities obtained.

| Sl. no.	Different hybrid materials	Adsorption capacity/density	Ions removed	Methods used	Isotherm supported	References
1	Fe(III)/La(III)-chitosan	$109 \, mg \, g^{-1}$	As(III) and As(V)	adsorption	–	[29]
2	Hybrid (polymeric/inorganic), fibrous sorbent, (FIBAN-As)	$75.67 \, mg \, g^{-1}$, $81.66 \, mg \, g^{-1}$	As(III) and As(V)	adsorption	Langmuir	[30]
3	Fe(II) loaded and Fe(III) loaded apricot, stone-based ACs	$2.023 \, mg \, g^{-1}$, $3.009 \, mg \, g^{-1}$	As(III) and As(V)	adsorption	Freundlich and Dubinin–Radushkevich	[31]
4	Al-HDTMA-sericite, (AH)	$0.433 \, mg \, g^{-1}$, $0.852 \, mg \, g^{-1}$	As(III) and As(V)	adsorption	Langmuir and Freundlich	[32]
5	Hydrous iron(III) oxide polyacrylamide	$43.0 \, mg \, g^{-1}$	As(V)	adsorption	–	[33]
6	GFH (granular ferric hydroxide)	$8 \, mg \, g^{-1}$	As(III)	adsorption	Freundlich	[34]
7	Laterite soil	$69.22 \, mg \, L^{-1}$	Total arsenic	adsorption	Langmuir, D–R	[35]
8	ZrPACM-43 (present material)	$0.20 \, mg \, g^{-1}$, $0.80 \, mg \, g^{-1}$	As(III)	adsorption	Freundlich, D–R	Present material
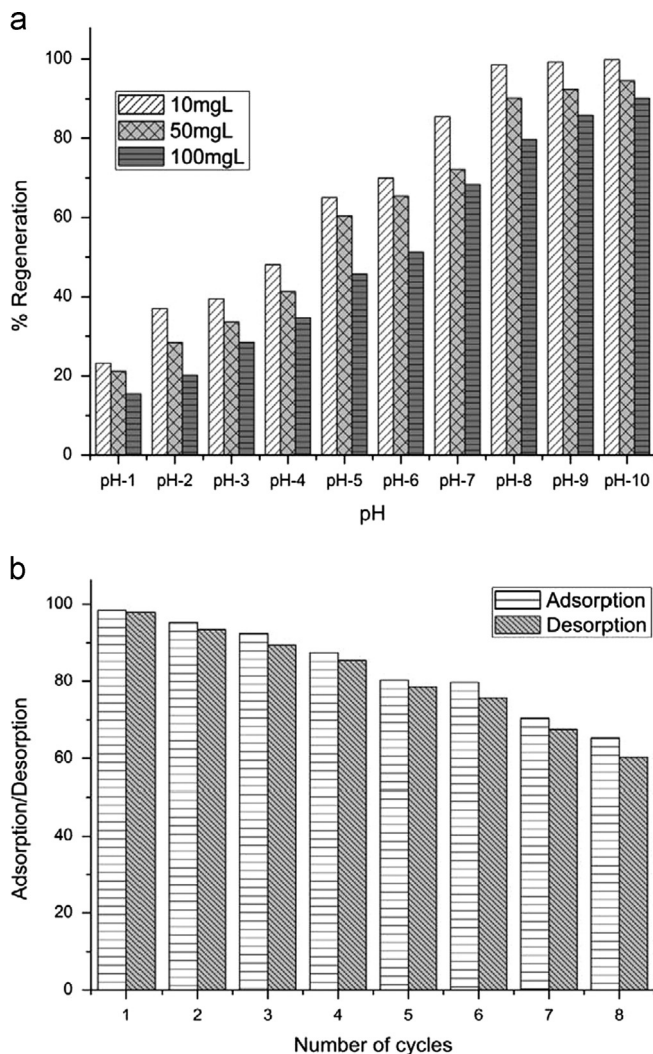
Fig. 12. Regeneration and reusability of the hybrid material ZrPACM-43: (a) regeneration percentage and (b) reusability of the hybrid material (experimental conditions: dose – 13 g L^{-1}, time: 120 min, temperature: 50 °C and strring speed: 20 r min^{-1}).

obtained for the hybrid material synthesized was 43 nm with maximum surface area of 341 m^2 g^{-1}. The maximum removal efficiency of arsenic(III) was 98.22% under optimum conditions of adsorbent dose 13 g L^{-1}, pH of the solution ≤ 5, contact time of 120 min and temperature 50 °C. The adsorption process followed second order kinetics with correlation coefficient of 0.999. The adsorption data are best supported to Freundlich model and D–R model with maximum adsorption capacity of 0.20 and 0.80 mg g^{-1}. The langmuir adsorption capacity was found to be 41.48 mg g^{-1}. The study of anion effect in the adsorption process shows that the adsorption decreases in order of anions; sulfate > chloride > carbonate > bicarbonate > nitrate. The regeneration study indicates that the material can be easily regenerated by using alkali at maximum pH of 10. The reusability study signifies that the material can be easily reused up to eight cycles with maximum removal of 60%. From the above study it is clearly concluded that the material can be suitably used for removal of arsenic.

Conflict of Interest

The authors declare no conflict of interest.

Acknowledgments

References

[1] D. Mohan, P. Charles, Arsenic removal from water/wastewater using adsorbents– a critical review, Journal of Hazardous Materials 142 (1–2) (2007) 1–53.

[2] Y.S.T. Choong, G.T. Chuah, H.Y Robia, L.F.G. Koay, I. Azni, Arsenic toxicity, health hazards and removal techniques from water: an overview, Desalination 217 (2007) 139–166.

[3] S. Shevade, R. Ford, Use of synthetic zeolites for arsenate removal from pollutant water, Water Research 38 (2004) 3197–3204.

[4] L. Lorenzen, J.S.J. Van Deventer, M.W. Landi, Factors affecting the mechanism of the adsorption of arsenic species on activated carbon, Minerals Engineering 8 (4) (1995) 557–569.

[5] F. Di. Natale, A. Erto, A. Lancia, D. Musmarra, Experimental and modelling analysis of As(V) ions adsorption on granular activated carbon, Water Research 42 (2008) 2007–2016.

[6] H.V. Aposhian, R.M. Maiorino, R.C. Dart, D.F Perry, Urinary excretion of meso-2, 3-dimercaptosuccinic acid in human subjects, Clinical Pharmacology & Therapeutics 45 (5) (1989) 520–526.

[7] IARC, Overall evaluation of carcinogenicity to humans. As evaluated in IARC monographs vol. 1–73, 1998, ⟨http://www.iarc. htm⟩ (updated November 30, 1998).

[8] WHO, Exposure to arsenic: a major public health concern, WHO Document Production Services, Geneva, Switzerland, 2010.

[9] EPA, Environmental Protection Agency, Environmental Pollution Control Alternatives, EPA/625/5-90/025, EPA/625/4-89/ 023, Cincinnati, US, 1990.

[10] M.J. Maushkar, Guidelines for water quality monitoring, Central pollution control board (A Government of India organisation), Delhi, India, 2007.

[11] BIS, (Bureau of Indian Standards) 10500, Indian Standard Drinking Water Specification; First revision, vol. 1–8, Bureau of Indian Standard Publication, New Delhi, India, 1991.

[12] S.W. Wan Ngah, C.L. Teong, M.K.A.M. Hanafiah, Adsorption of dyes and heavy metal ions by chitosan composites a review, Carbohydrate Polymers 83 (2011) 1446–1456.

[13] A. Afkhami, M. Saber-Tehrani, H. Bagheri, Simultaneous removal of heavy-metal ions in wastewater samples using nano-alumina modified with 2,4-dinitrophenylhydrazine, Journal of Hazardous Materials 181 (2010) 836–844.

[14] Z. Wu, M. He, X. Guo, R. Zhou, Removal of antimony(III) and antimony(V) from drinking water by ferric chloride coagulation: competing ion effect and the mechanism analysis, Separation and Purification Technology 76 (2010) 184–190.

[15] R.K. Misra, S.K. Jain, P.K. Khatri, Iminodiacetic acid functionalized cation exchange resin for adsorptive removal of Cr(VI), Cd (II), Ni(II) and Pb(II) from their aqueous solutions, Journal of Hazardous Materials 185 (2011) 1508–1512.

[16] F. Fernane, M.O. Mecherri, P. Sharrock, M. Hadioui, H. Lounici, M. Fedoroff, Sorption of cadmium and copper ions on natural and synthetic hydroxylapatite particles, Materials Characterization 59 (2008) 554–559.

[17] A. Dabrowski, Z. Hubicki, P. Podkościelny, E. Robens, Selective removal of the heavy metal ions from waters and industrial wastewaters by ion-exchange method, Chemosphere 56 (2004) 91–106.

[18] S.K. Nataraj, K.M. Hosamani, T.M. Aminabhavi, Nanofiltration and reverse osmosis thin film composite membrane module for the removal of dye and salts from the simulated mixtures, Desalination 249 (2009) 12–17.

[19] N.H Tran, A.J. Hartmann, R.N. Lamb, Structural order of nanocrystalline ZnO films, Journal of Physical Chemistry B 21 (1999) 4264–4268.

[20] G. Alberti, E. Torracca, A. Conte, Journal of Inorganic and Nuclear Chemistry 28 (1966) 607.

[21] F. Amiri, M.M. Rahman, H. Bornick, E. Worch, Sorption behaviour of phenols on natural sandy aquifer material during flow-through column experiments: the effect of pH, Acta Hydrochimica et Hydrobiologica 32 (3) (2004) 214–224.

[22] S. Lagergren, To the theory of so-called adsorption of dissolved substances, The Royal Swedish Academy of Sciences 24 (1889) 1–39.

[23] J. Wang, L. Zhao, Han L. Duan, Y. Chen, Adsorption of aqueous Cr(VI) by novel fibrous adsorbent W with amino and quaternary ammonium groups, Industrial and Engineering Chemistry Research 51 (2012) 13655–13662.

[24] P.V. Messina, P.C. Schulz, Adsorption of reactive dyes on titania–silica mesoprous materials, Journal of Colloid and Interface Science 299 (2006) 305–320.

[25] C. Namasivayam, R.T. Yamuna, Adsorption of direct red 12 B by biogas residual slurry: equilibrium and rate processes, Environmental Pollution 89 (1995) 1–7.

[26] Langmuir, The adsorption of gases on plane surfaces of glass, mica, and platinum, Journal of the American Chemical Society 40 (9) (1918) 1361–1403.

[27] H. Freundlich, About the adsorption in solutions, Zeitschrift für Physikalische Chemie 57 (1906) 384–470.

[28] C. Raji, T.S. Anirudhan, Batch Cr (VI) removal by polyacrylamide grafted sawdust: kinetics and thermodynamics, Water Research 32 (12) (1998) 3772–3780.

[29] R.N. Shinde, A.K. Pandey, R. Acharya, R. Guin, S.K. Das, N.S. Rajurkar, P.K. Pujari, Chitosan-transition metal ions complexes for selective arsenic(V) preconcentration, Water Research 47 (2013) 3497–3506.

[30] O.M. Vatutsina, V.S. Soldatov, V.I. Sokolova, J. Johann, M. Bissen, A. Weissenbacher, A new hybrid (polymer/inorganic) fibrous sorbent for arsenic removal from drinking water, Reactive and Functional Polymers 67 (2007) 184–2001.

[31] Tuna Hunter (Avc) Ozge Asli, Ozdemir Ercan, Lightning(Şimşek) Bilgin Esra, Cup (Beker) Ulker, Removal of As(V) from aqueous solution by activated carbon-based hybrid adsorbents: impact of experimental conditions, Chemical Engineering Journal, 223, 116–128.

[32] D. Tiwari, S.M. Lee, Novel hybrid materials in the remediation of ground waters contaminated with As(III) and As(V), Chemical Engineering Journal 204–206 (2012) 23–31.

[33] Y. Shigetomi, Y. Hori, T. Kojima, The removal of arsenate in waste water with an adsorbent prepared by binding hydrous iron(III) oxide with polyacrylamide, Bulletin of the Chemical Society of Japan 53 (1980) 1475–1476.

[34] M. Badruzzaman, P. Westerhoff, D.R.U. Knappe, Intraparticle diffusion and adsorption of arsenate onto granular ferric hydroxide (GFH), Water Research 38 (18) (2004) 4002–4012.

[35] S.K. Maji, A. Pal, T. Pal, Arsenic removal from real-life groundwater by adsorption on laterite soil, Journal of Hazadous Materials 151 (2–3) (2008) 811–820.